Thermal Generation of Spin Current in an Antiferromagnet

S. Seki,[1,2] T. Ideue,[3] M. Kubota,[1,4,*] Y. Kozuka,[3] R. Takagi,[1] M. Nakamura,[1] Y. Kaneko,[1] M. Kawasaki,[1,3] and Y. Tokura[1,3]
[1]RIKEN Center for Emergent Matter Science (CEMS), Wako 351-0198, Japan
[2]PRESTO, Japan Science and Technology Agency (JST), Tokyo 102-8666, Japan
[3]Department of Applied Physics and Quantum Phase Electronics Center (QPEC), University of Tokyo, Tokyo 113-8656, Japan
[4]Research and Development Headquarters, ROHM Co., Ltd., Kyoto 615-8585, Japan

(Received 11 August 2015; revised manuscript received 31 October 2015; published 29 December 2015)

The longitudinal spin Seebeck effect has been investigated for a uniaxial antiferromagnetic insulator Cr_2O_3, characterized by a spin-flop transition under magnetic field along the c axis. We have found that a temperature gradient applied normal to the Cr_2O_3/Pt interface induces inverse spin Hall voltage of spin-current origin in Pt, whose magnitude turns out to be always proportional to magnetization in Cr_2O_3. The possible contribution of the anomalous Nernst effect is confirmed to be negligibly small. The above results establish that an antiferromagnetic spin wave can be an effective carrier of spin current.

DOI: 10.1103/PhysRevLett.115.266601 PACS numbers: 72.25.Mk, 65.40.-b, 75.30.Ds, 75.70.-i

Spin current, i.e., a flow of spin angular momentum or magnetic moment, has recently attracted revived attention as the potential alternative to charge current with improved energy efficiency [1–6]. Spin-polarized conduction electrons in metallic systems, as well as spin waves in insulating systems, are considered the two important carriers of spin current [7,8]. Especially, the latter spin-wave spin current (SWSC) has much longer decay length and can avoid the simultaneous flow of charge current accompanied with Joule heat loss, which are strong advantages for the spintronics applications.

In the case of ferro- or ferrimagnetic insulators (FMI), SWSC can be generated by various external stimuli such as magnetic resonance [7,9] or application of temperature gradient ∇T [8,10–14]. The latter process is called the spin Seebeck effect, and the simultaneous application of ∇T and magnetic field H to FMI induces SWSC carrying spin angular momentum $\vec{\sigma}$ ($\parallel \vec{H}$). When paramagnetic metal (PM) is attached to FMI, the spin current $\vec{J}_s$ flowing normal to their interface plane is injected into the PM layer through the interfacial spin-exchange interaction [11–14]. This causes the inverse spin Hall effect and associated electric voltage $V_{\rm ISHE}$ in PM, which is given by

$$\vec{V}_{\rm ISHE} \propto L_V \theta_{\rm SH} (\vec{J}_s \times \vec{\sigma}). \quad (1)$$

Here, $\theta_{\rm SH}$ is the spin Hall angle of PM, and L_V is the gap distance between the electrodes for the voltage measurement. This process can be viewed as a kind of thermoelectric conversion with its efficiency scaling with the film size L_V, which may offer a unique route for waste heat utilization without requiring a series connection of thermocouples [15].

Previously, the studies of SWSC have mainly focused on a limited number of ferrimagnetic insulators [11] such as rare-earth iron garnet $R_3Fe_5O_{12}$ [including $Y_3Fe_5O_{12}$ (YIG)] [8] and spinel ferrite MFe_2O_4 (M is a $3d$ transition metal) [16]. However, most magnetic insulators are rather antiferromagnetic [17], and it is a crucial issue whether the spin waves in antiferromagnets can carry spin current or not. Since the energy gap of spin wave (i.e., the frequency of magnetic resonance) for antiferromagnets is characterized by a 2 or 3 orders of magnitude larger value than those for ferromagnets [18,19], the antiferromagnetic spin wave can potentially serve as the medium for ultrafast information processing and communications. Antiferromagnets are also free from stray fields in the ground state, which implies that their dynamics are relatively robust against magnetic perturbations or defects. In general, an antiferromagnetic spin wave is described as the propagating precession of two oppositely aligned sublattice magnetic moments [18,19]. Recent theoretical studies have suggested that such local spin oscillations are represented by two degenerated magnon branches carrying opposite sign of spin angular momentum in the limit of $H \rightarrow 0$ [20], where the total spin current will cancel out for the thermal excitation process [21]. Experimentally, antiferromagnets have been investigated as the potential spin transport layer [22] but never employed as the source of spin current.

In this Letter, we report the experimental observation of the spin Seebeck effect for a uniaxial antiferromagnetic insulator Cr_2O_3. By applying a temperature gradient normal to the Cr_2O_3/Pt interface, the inverse spin Hall voltage of spin-current origin has successfully been detected in the Pt layer. The magnitude of thermally induced spin current turns out to be always proportional to magnetization in Cr_2O_3 even under the H-induced spin-flop transition, which proves that an antiferromagnetic spin wave can be an effective carrier of spin current.

Bulk single crystals of Cr_2O_3 were grown by the laser floating zone method [23]. They are cut into rectangular shape and polished with diamond slurry and colloidal

 © 2015 American Physical Society

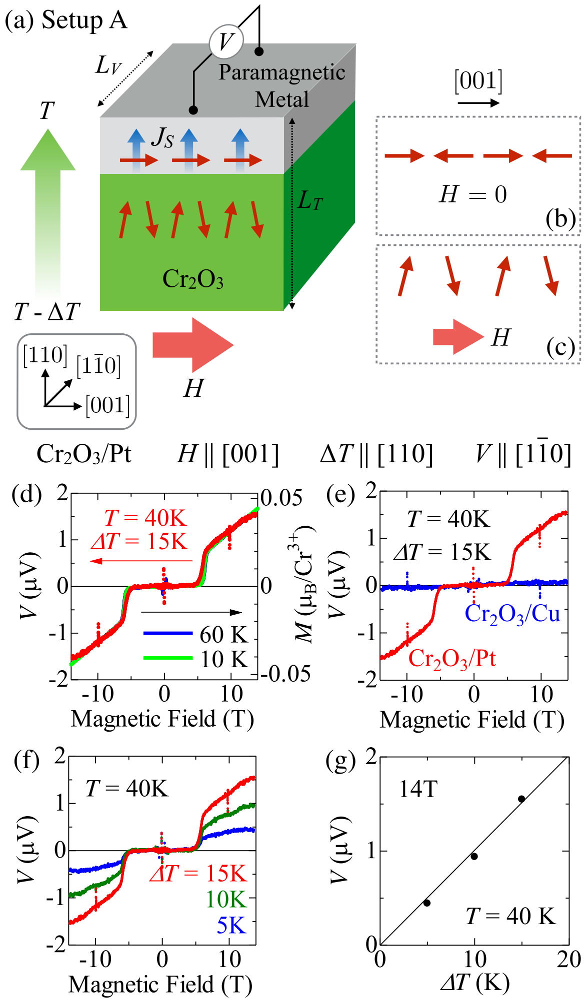

FIG. 1 (color online). (a) Experimental setup for the measurement of the longitudinal spin Seebeck effect, with magnetic field (H) applied along the [001] axis of Cr_2O_3. Arrows in Cr_2O_3 represent the local magnetic moments, and bold blue (thin red) arrows in paramagnetic metal correspond to the propagation direction (carried spin angular momentum) of the associated spin current J_s. L_T (thickness of bulk Cr_2O_3 along the temperature gradient direction) and L_V [distance between the electrodes (black circles) on the metal layer] are 0.5 and 4 mm, respectively. Unless specified, Pt is employed as the paramagnetic metal. (b), (c) The magnetic structures of Cr_2O_3 for the ground state (i.e., $H = 0$) and the H-induced spin-flopped state, respectively. (d) H dependence of induced electric voltage V for Pt and magnetization M for Cr_2O_3. The similar voltage profiles are also measured with (e) a different paramagnetic metal (Cu) and (f) different magnitudes of temperature gradient ΔT. (g) ΔT dependence of Pt voltage at 14 T.

silica. On the polished surface of Cr_2O_3, a thin film of Pt (10 nm) or Cu (20 nm) is deposited as the PM layer by the radio-frequency sputtering method. To provide the appropriate temperature gradient ∇T, the sample is sandwiched with a pair of Cu blocks (covered by thin Al_2O_3 film to guarantee the electrical insulation but with good thermal contact) under the high vacuum condition less than 10^{-4} Torr. One Cu block serves as the thermal bath with temperature $T - \Delta T$, and another Cu block is equipped with a resistive heater to keep its temperature T. Their temperatures are actively monitored and controlled by Cernox thermometers and a Lake Shore 335 temperature controller. Here, the temperature gradient is given by $\nabla T = \Delta T / L_T$ with L_T being the sample thickness along the temperature gradient direction. To evaluate the magnitude of thermally induced J_s through Eq. (1), H dependence of raw electric voltage V_{raw} is measured in the PM layer with and without ∇T by nanovoltmeter. After the subtraction of background (i.e., the one with $\Delta T = 0$), the H-odd component of induced voltage V is extracted by $V(H,\Delta T) = \{[V_{raw}(H,\Delta T) - V_{raw}(H,0)] - [V_{raw}(-H,\Delta T) - V_{raw}(-H,0)]\}/2$. Magnetization M and thermal conductivity κ for Cr_2O_3 are measured with the Physical Properties Measurement System (PPMS, Quantum Design Inc).

The target compound Cr_2O_3 has a corundum crystal structure with trigonal space group $R\bar{3}c$. The magnetism is dominated by the Cr^{3+} ion with $S = 3/2$, and the antiferromagnetic order with local magnetic moments pointing along the [001] axis is stabilized below the Néel temperature $T_N \sim 308$ K [Fig. 1(b)]. Since antiferromagnetically aligned spins prefer to lie normal to H, the application of $H \| [001]$ larger than the critical field value H_c induces spin-flop transition and reorients the magnetic moment direction as shown in Fig. 1(c) [24,25].

In the following, we mainly discuss the results for the Cr_2O_3/Pt sample under the experimental configuration shown in Fig. 1(a) (i.e., setup A) unless specified. Here, Pt is deposited on the (110) plane of Cr_2O_3 and ∇T is applied normal to it, which corresponds to the geometry of the longitudinal spin Seebeck effect [12,13]. Magnetic field is applied along the [001] direction of Cr_2O_3. To detect the electric voltage of spin-current origin following Eq. (1), the V component normal to H is measured within the Pt layer. Figure 1(d) indicates the magnetic field dependence of M for Cr_2O_3, as well as V in the Pt layer at $T = 40$ K and $\Delta T = 15$ K. The application of $H \| [001]$ larger than $H_c \sim 6$ T causes a spin-flop transition and magnetization step in the $M - H$ profile, which remains almost T independent below 60 K. Correspondingly, a clear steplike enhancement of V is observed at H_c. The magnitude of V in Pt is found to be proportional to M in Cr_2O_3, suggesting that the observed voltage originates from thermally induced spin current mediated by an antiferromagnetic spin wave carrying nonzero spin angular momentum $\sigma \propto M$. Such a correspondence is also observed for the case of $H \| [1\bar{1}0]$, where a spin-flop transition is absent and both V and M show H-linear behavior (see the Supplemental Material [26]).

To further establish the validity of Eq. (1) in this system, the same voltage measurement is performed for the Cr_2O_3/Cu sample [Fig. 1(e)]. The obtained V in the Cu layer is negligibly small, consistent with the much smaller

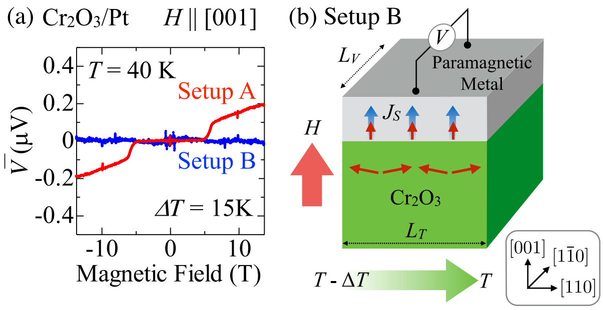

FIG. 2 (color online). (a) Magnetic field dependence of the normalized Pt voltage $\bar{V}$ $(= VL_T/L_V)$ for H applied along the [001] axis of Cr_2O_3, measured with setup A [i.e., Fig. 1(a)] and setup B as shown in (b). For the latter case, L_T and L_V are 2 and 4 mm, respectively, and only the anomalous Nernst effect can contribute to the induced voltage.

spin Hall angle for Cu($\theta_{SH} \sim 0.003$) than that for Pt($\theta_{SH} \sim 0.1$) [29]. The measurements are also performed under different magnitudes of ΔT for the Cr_2O_3/Pt sample while keeping $T = 40$ K [Fig. 1(f)]. Figure 1(g) summarizes the ΔT dependence of the V value at $H = 14$ T, and V turns out to be proportional to ΔT. Previously, the relationship $J_s \propto \nabla T$ has been proposed for several ferromagnetic materials such as YIG [12,30], and our present results suggest that it also holds for antiferromagnets.

For the YIG/Pt system, the possible contribution of the anomalous Nernst effect (ANE) into the H-odd voltage component has recently been discussed [13,31]. This scenario assumes the proximity ferromagnetism in the Pt layer (with local magnetization M_{Pt}) at the interface with YIG, and the ANE contribution to the voltage is given by

$$\vec{V}_{ANE} \propto L_V(\vec{M}_{Pt} \times \vec{\nabla} T). \quad (2)$$

In the case of setup A [Fig. 1(a)], the observed voltage comprises $V = V_{ISHE} + V_{ANE}$, and thus the subtraction of V_{ANE} is necessary to extract the pure contribution of V_{ISHE}. To estimate the magnitude of V_{ANE}, we employed a different experimental setup as shown in Fig. 2(b) (i.e., setup B). Here, Pt is deposited on the (001) plane of Cr_2O_3 and H is applied perpendicular to it. ∇T is along the in-plane [110] direction, and the voltage component normal to both ∇T and H is measured within the Pt layer. In setup B, V_{ISHE} becomes 0 due to $\vec{J}_s \| \vec{\sigma}$ and only V_{ANE} can contribute to the observed voltage [13]. In Fig. 2(a), the H dependence of $\bar{V}$ $(= VL_T/L_V)$, i.e., voltage normalized with sample dimensions, is plotted for the Cr_2O_3/Pt sample with both setups A and B. While H induces the spin-flop transition at 6 T in Cr_2O_3 for both configurations, the discernible voltage signal in Pt is observed only for setup A. This proves that the contribution of V_{ISHE} (i.e., the longitudinal spin Seebeck effect) is dominant and V_{ANE} is negligibly small in the present sample [32].

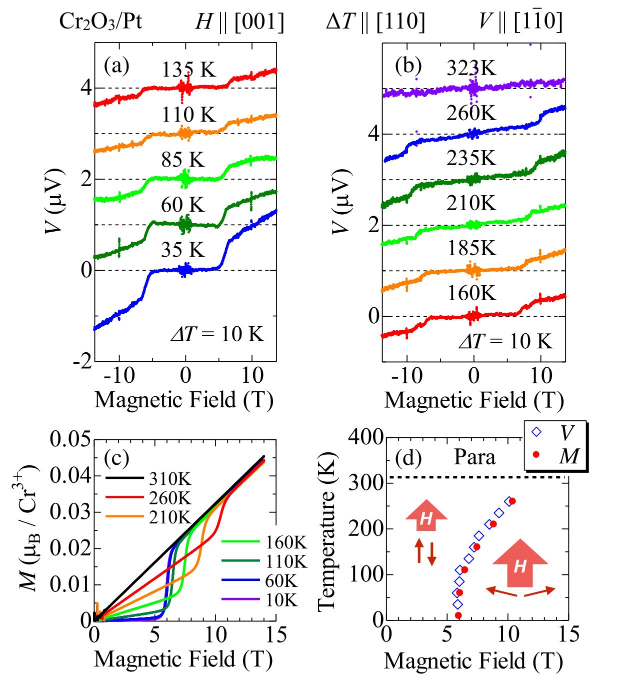

FIG. 3 (color online). (a),(b) Magnetic field dependence of Pt voltage measured at various temperatures T for setup A [i.e., Fig. 1(a)], with the constant temperature gradient $\Delta T = 10$ K. (c) The corresponding magnetic field dependence of magnetization for Cr_2O_3 with $H \| [001]$. (d) $H - T$ phase diagram for Cr_2O_3 with $H \| [001]$, deduced from anomalies in magnetization profile (red closed circles). Above $T_N \sim 308$ K, Cr_2O_3 becomes paramagnetic. The steplike anomalies for Pt voltage observed in (a) and (b) are also plotted as blue open diamonds.

Next, we investigated the temperature dependence of voltage profiles for the Cr_2O_3/Pt sample with the original setup A. Figures 3(a) and 3(b) indicate the H dependence of V in the Pt layer, measured at various temperatures keeping $\Delta T = 10$ K. The corresponding H dependence of M for Cr_2O_3 obtained at various T is also plotted in Fig. 3(c). Both V for Pt and M for Cr_2O_3 show a clear steplike anomaly corresponding to the spin-flop transition at H_c. Based on these measurements, the $H - T$ magnetic phase diagram for Cr_2O_3 under $H \| [001]$ is summarized in Fig. 3(d) [25]. While H_c becomes larger for higher temperature, the anomalies in V and M always coincide with each other. This confirms that the observed V in Pt clearly reflects the magnetic nature of the underlying Cr_2O_3. In Fig. 4, the magnitudes of V and M obtained at 14 T are plotted as a function of temperature. The V value shows clear enhancement for lower T, while the corresponding M value at 14 T remains almost unchanged for whole temperature range. A similar increase of V for lower T has recently been reported for YIG/Pt, for which several different mechanisms have been proposed. One candidate is the phonon-drag mechanism [11,35,36], where thermally induced propagating phonons drag magnons through a magnon-phonon interaction. This model assumes that

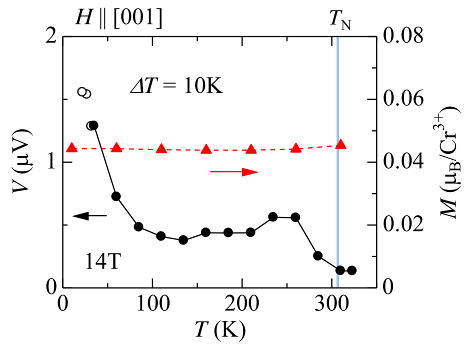

FIG. 4 (color online). Temperature dependence of the inverse spin Hall voltage for the Cr_2O_3/Pt system at 14 T, obtained from the data in Figs. 3(a) and 3(b) measured with $\Delta T = 10$ K (black closed circles). The additional set of data obtained with $\Delta T = 5$ K, which is scaled using the relationship $V \propto \Delta T L_V/L_T$, is shown as black open circles. Corresponding magnetization values for Cr_2O_3 at 14 T, obtained from the data in Fig. 3(c), are also plotted as red triangles.

prolonged phonon lifetime in the lower-T region enhances the magnitude of J_s, and such an enhancement of phonon lifetime has been observed for the present Cr_2O_3 through the thermal conductivity measurement (see the Supplemental Material [26]). However, another theoretical model has proposed that the T dependence of thermally induced spin current rather reflects the nature of magnon dispersion and the energy dependence of magnon-electron interaction [37]. To fully understand the mechanism behind the observed T dependence, further theoretical and experimental investigations would be essential. Above $T_N \sim 308$ K, the magnitude of V is gradually suppressed. The small but nonzero V signal at 323 K may be relevant with the short-range spin correlation in the paramagnetic state [38].

In general, simple uniaxial antiferromagnets are characterized by two degenerated magnon branches with dispersion relationship $E^+(k)$ and $E^-(k)$, which are expected to carry opposite sign of spin angular momentum [20,21]. This degeneracy is lifted under H applied along the magnetic easy axis, where $E^+(k)$ [$E^-(k)$] linearly increases [decreases] as a function of H. When $E^-(k)$ reaches 0 at $H = H_c$, the spin-flopped state characterized by two different magnon branches carrying the same sign of spin angular momentum is stabilized [19]. Since the thermal process excites magnon modes of any wave number k and energy E following the Bose distribution function [39], ∇T-induced generation of nonzero spin current is always justified for antiferromagnets with finite H. Note that the energy gap of an antiferromagnetic spin wave typically ranges from the order of 1 to 10 meV (i.e., the order of 100 GHz to THz in terms of magnetic resonance frequency), which is much higher than that of the ferromagnetic one in the order of 0.01 meV [19]. In the case of Cr_2O_3, the energy gap of an antiferromagnetic spin wave is 0.7 meV [$= E^{\pm}(0)$] in the ground state, according to the previous magnetic resonance experiments [40,41]. Considering that 1 K of thermal energy corresponds to 0.086 meV (based on the relationship $E = k_B T$ with k_B being the Boltzmann constant), such antiferromagnetic spin waves can be easily excited through the thermal process for the presently employed temperature range. Recent theories predict that each of two degenerated antiferromagnetic magnon branches for $H \to 0$ is also active for a circularly polarized microwave but with opposite handedness [20,42], and the efficient optical generation of spin current through selective mode excitation under zero magnetic field would be an interesting challenge for antiferromagnets [43].

In summary, we have experimentally observed the longitudinal spin Seebeck effect for a uniaxial antiferromagnetic insulator Cr_2O_3. The application of temperature gradient normal to the Cr_2O_3/Pt interface causes the inverse spin Hall voltage of spin-current origin in the Pt layer, whose magnitude turns out to be proportional to magnetization M in Cr_2O_3. The present finding demonstrates that the antiferromagnetic spin wave can be an efficient carrier of spin current, which highlights antiferromagnetic insulators as the promising source of unique spintronic functions.

The authors thank T. Arima, K. S. Takahashi, Y. Iwasa, Y. Kasahara, H. Matsui, Y. Tokunaga, A. Kikkawa, Y. Ohnuma, Y. Shiomi, K. Uchida, and E. Saitoh for enlightening discussions and experimental help. This work was partly supported by the Mitsubishi Foundation, Grants-in-Aid for Scientific Research (Grants No. 26610109 and No. 15H05458) from the MEXT of Japan, and the FIRST Program by the Japan Society for the Promotion of Science (JSPS).

Note added.—Recently, we became aware of similar results for MnF_2 film by Wu *et al.* [44].

*Present address: Corporate Technology and Business Development Unit, Murata Manufacturing Co., Ltd., Nagaokakyo, Kyoto 617-8555, Japan.

[1] S. Maekawa *et al.*, *Spin Current* (Oxford University Press, New York, 2012).
[2] G. E. W. Bauer, E. Saitoh, and B. J. Wees, Nat. Mater. **11**, 391 (2012).
[3] S. R. Boona, R. C. Myers, and J. P. Heremans, Energy Environ. Sci. **7**, 885 (2014).
[4] S. Murakami, N. Nagaosa, and S. C. Zhang, Science **301**, 1348 (2003).
[5] Y. K. Kato *et al.*, Science **306**, 1910 (2004).
[6] J. E. Hirsch, Phys. Rev. Lett. **83**, 1834 (1999).
[7] Y. Kajiwara *et al.*, Nature (London) **464**, 262 (2010).
[8] K. Uchida *et al.*, Nat. Mater. **9**, 894 (2010).
[9] E. Saitoh, M. Ueda, H. Miyajima, and G. Tatara, Appl. Phys. Lett. **88**, 182509 (2006).

[10] K. Uchida, S. Takahashi, K. Harii, J. Ieda, W. Koshibae, K. Ando, S. Maekawa, and E. Saitoh, Nature (London) **455**, 778 (2008).
[11] K. Uchida, T. Ota, H. Adachi, J. Xiao, T. Nonaka, Y. Kajiwara, G. E. W. Bauer, S. Maekawa, and E. Saitoh, J. Appl. Phys. **111**, 103903 (2012).
[12] K. Uchida, H. Adachi, T. Ota, H. Nakayama, S. Maekawa, and E. Saitoh, Appl. Phys. Lett. **97**, 172505 (2010).
[13] T. Kikkawa, K. Uchida, Y. Shiomi, Z. Qiu, D. Hou, D. Tian, H. Nakayama, X. F. Jin, and E. Saitoh, Phys. Rev. Lett. **110**, 067207 (2013).
[14] H. Adachi, K. Uchida, E. Saitoh, and S. Maekawa, Rep. Prog. Phys. **76**, 036501 (2013).
[15] A. Kirihara, K. Uchida, Y. Kajiwara, M. Ishida, Y. Nakamura, T. Manako, E. Saitoh, and S. Yorozu, Nat. Mater. **11**, 686 (2012).
[16] K. Uchida, T. Nonaka, T. Ota, and E. Saitoh, Appl. Phys. Lett. **97**, 262504 (2010).
[17] M. Imada, A. Fujimori, and Y. Tokura, Rev. Mod. Phys. **70**, 1039 (1998).
[18] F. Keffer and C. Kittel, Phys. Rev. **85**, 329 (1952).
[19] S. Foner, *Antiferromagnetic and Ferrimagnetic Resonance*, Magnetism Vol. 1 (Academic, New York, 1963), p, 383.
[20] R. Cheng, J. Xiao, Q. Niu, and A. Brataas, Phys. Rev. Lett. **113**, 057601 (2014).
[21] Y. Ohnuma, H. Adachi, E. Saitoh, and S. Maekawa, Phys. Rev. B **87**, 014423 (2013).
[22] H. Wang, C. Du, P. C. Hammel, and F. Yang, Phys. Rev. Lett. **113**, 097202 (2014).
[23] T. Ito, T. Ushiyama, Y. Yanagisawa, Y. Tomioka, I. Shindo, and A. Yanase, J. Cryst. Growth **363**, 264 (2013).
[24] M. Fiebig, D. Fröhlich, and H.-J. Thiele, Phys. Rev. B **54**, R12681 (1996).
[25] R. D. Yacovitch and Y. Shapira, Physica (Amsterdam) **86–88B+C**, 1126 (1977).
[26] See Supplemental Material at http://link.aps.org/supplemental/10.1103/PhysRevLett.115.266601, which includes Refs. [27,28], for details.
[27] N. W. Ashcroft and N. D. Mermin, *Solid State Physics* (Holt-Saunders, New York, 1976).
[28] J. M. Jolivet, A. M. de Goer, and A. de Combarieu, J. Phys. Colloques **39**, C6-990 (1978).
[29] H. L. Wang, C. H. Du, Y. Pu, R. Adur, P. C. Hammel, and F. Y. Yang, Phys. Rev. Lett. **112**, 197201 (2014).
[30] S. R. Boona and J. P. Heremans, Phys. Rev. B **90**, 064421 (2014).
[31] S. Y. Huang, X. Fan, D. Qu, Y. P. Chen, W. G. Wang, J. Wu, T. Y. Chen, J. Q. Xiao, and C. L. Chien, Phys. Rev. Lett. **109**, 107204 (2012).
[32] In the case of YIG/Pt with the similar ∇T value, the inverse spin Hall voltage of $\bar{V} \sim 3\ \mu$V has been reported in the saturated ferrimagnetic state at room temperature [13]. Considering the relatively small magnitude of induced M (less than 2% of saturated magnetization) and the $\bar{V} \propto M$ relationship observed for the thermal excitation process [Fig. 1(d)], the presently obtained $\bar{V} \sim 0.2\ \mu$V for Cr_2O_3/Pt at 14 T for 40 K may not be so small. To make a reasonable comparison, however, various factors such as the difference of spin mixing conductance [33], magnon decay length [34], magnon dispersion, as well as their T and H dependence must be further considered.
[33] M. Weiler *et al.*, Phys. Rev. Lett. **111**, 176601 (2013).
[34] A. Kehlberger *et al.*, Phys. Rev. Lett. **115**, 096602 (2015).
[35] H. Adachi, K. Uchida, E. Saitoh, J. Ohe, S. Takahashi, and S. Maekawa, Appl. Phys. Lett. **97**, 252506 (2010).
[36] C. M. Jaworski, J. Yang, S. Mack, D. D. Awschalom, R. C. Myers, and J. P. Heremans, Phys. Rev. Lett. **106**, 186601 (2011).
[37] H. Jin, S. R. Boona, Z. Yang, R. C. Myers, and J. P. Heremans, Phys. Rev. B **92**, 054436 (2015).
[38] S. M. Wu, Phys. Rev. Lett. **114**, 186602 (2015).
[39] C. Kittel, *Quantum Theory of Solids* (Wiley, New York, 1963).
[40] E. S. Dayhoff, Phys. Rev. **107**, 84 (1957).
[41] S. Foner, Phys. Rev. **130**, 183 (1963).
[42] T. Satoh, S. J. Cho, R. Iida, T. Shimura, K. Kuroda, H. Ueda, Y. Ueda, B. A. Ivanov, F. Nori, and M. Fiebig, Phys. Rev. Lett. **105**, 077402 (2010).
[43] The thermal generation of spin current in antiferromagnets requires finite magnitude of magnetic field, and the effect of a stray field may not be completely avoided, while the magnitude of H-induced M in Cr_2O_3 at 14 T is just less than 2% of saturation value. To obtain the spin current in antiferromagnets under zero magnetic field, the selective magnon mode excitation by a circularly polarized microwave will be promising [20].
[44] S. M. Wu *et al.*, arXiv:1509.00439.